AIAA 82-4015

Growth of Two-Dimensional Wakes Behind Solid and Porous Strips

Donald D. Gray* and Gerard F. Sheldon†
Purdue University, West Lafayette, Ind.

Nomenclature

c = chord (strip width normal to flow)
d = diameter
ℓ = characteristic length scale for two-dimensional wakes (distance from central plane where axial velocity defect is $0.6 \times$ centerline defect)
L = characteristic length scale for axisymmetric wakes (radius where axial velocity defect is $0.607 \times$ centerline defect)
r = correlation coefficient
U = axial mean velocity
U_c = centerline axial mean velocity
U_∞ = freestream velocity
ΔU = $U_\infty - U$ (velocity defect)
x = downstream distance from object
x_0 = downstream distance from object to virtual origin
x' = $x - x_0$ (downstream distance from virtual origin)
y = distance normal to the central plane
β = porosity (ratio of open area to total area)
θ = momentum thickness

Introduction

BASED on a comparison of the axisymmetric turbulent wakes behind a sphere and a porous disk, Bevilaqua and Lykoudis[1] concluded that far wake entrainment rates are strongly influenced by large eddies whose production depends on the shape of the drag producing body. This Note presents data which support the validity of the Bevilaqua-Lykoudis hypothesis in two-dimensional wakes.

The nature of the entrainment process in unbounded flows such as plumes, jets, and wakes has been a source of continuing conjecture and controversy. Simple eddy viscosity or mixing length models imply that the mean velocity field (and hence the entrainment rate) depends only on a few gross flow parameters for each particular flow geometry. Thus the mean velocity field of axisymmetric or two-dimensional far wakes is predicted to depend only on the fluid density, the freestream velocity, and the drag on the wake producing object. Appropriate normalization should then reveal the same mean flow representation for all flows of a particular type, e.g., two-dimensional far wakes. When this hypothesis is tested using data obtained behind various circular cylinders, it is verified, aside from a virtual origin correction.[2,3] The foregoing argument implies that the exact shape of the drag producing object will not influence the mean far wake. Hence the normalized mean far wakes behind circular cylinders or flat strips should be indistinguishable. This conclusion may be rationalized by assuming either that the turbulence behind various obstacles achieves a universal structure or that such differences as may persist have no effect on the mean flow.

Received Feb. 23, 1981; revision received July 20, 1981.

*Assistant Professor of Hydromechanics, School of Civil Engineering.

†Graduate Research Assistant, School of Civil Engineering, presently: Engineer, Union Carbide Corporation, Linde Division, Tonawanda, N.Y.

Bevilaqua and Lykoudis[1] rejected these arguments after comparing the wakes of a sphere and a porous disk mounted normal to the freestream in a wind tunnel. The disk was fabricated of 18 mesh metal screen and had the same diameter as the sphere. The disk porosity (ratio of open area to total area) of 0.82 was chosen to produce equal drags at the test Reynolds number of 10,000.

Using a hot film anemometer, Bevilaqua and Lykoudis measured profiles of mean velocity, turbulence intensity, intermittency, and principal stress out to 110 diam. Behind the sphere the mean velocity and turbulence intensity profiles approached their self-preserving forms within 5 diam, and periods of nonturbulent flow (intermittency) occurred on the wake centerline beyond 15 diam. Unlike the sphere, the near wake of the porous disk did not contain a recirculation zone. The mean velocity and turbulence intensity profiles behind the porous disk became self-preserving after 20 diam, and the flow on the wake centerline remained fully turbulent for more than 100 diam. The explanation of these results was based on a dye injection visualization[4] of the wake behind a towed sphere in water. This revealed a large scale snaking pattern of alternating bulges and hollows which caused intermittency on the wake centerline. The bulges were seen to be large scale vortical structures. In contrast, the wake of the porous disk was far less contorted and showed no large scale snaking.

Bevilaqua[5] fitted power laws to the normalized length scales measured in the wind tunnel and found much more rapid spread behind the sphere.

$$L/\theta = 0.73(x'/\theta)^{0.333} \quad \text{(sphere)}$$

$$= 0.37(x'/\theta)^{0.333} \quad \text{(porous disk, } \beta = 0.82\text{)} \qquad (1)$$

To summarize, Bevilaqua and Lykoudis found that both mean velocity fields had the same self-preserving functional form but had distinctly different turbulence structures and grew at dramatically different rates. These findings, coupled with the flow visualization results, led Bevilaqua and Lykoudis to conclude that the persistent large eddies shed by the sphere play an important role in enhancing far wake entrainment. Recalling the observations of persistent large scale vortical structures in the mixing layer[6] and behind the circular cylinder,[7] they speculated that the presence or absence of large scale vortices could have a decisive effect on the rate of entrainment in all free turbulent flows.

This rather radical hypothesis should be repeatedly tested, especially because turbulent axisymmetric wakes eventually relaminarize.[8,9] Consequently the present authors decided to compare the two-dimensional far wakes behind solid and porous obstacles.

The only previous research on such wakes was performed by Castro[10] who studied the near wake region behind solid and perforated strips mounted normal to the airstream of a low-speed wind tunnel. Eleven strips, with lengths of 61 cm, widths (chords) of 4.13 cm, and porosities ranging from 0 to 0.645, were used. Tests were conducted at Reynolds numbers between 25,000 and 90,000 based on freestream velocity, chord, and kinematic viscosity. Measurements of drag coefficient, eddy shedding frequency, and centerline mean velocity and turbulence intensity were obtained for $x/c \leq 20$.

Castro discovered that a zone of recirculating flow was attached to the back of the solid strip but was displaced successively farther downstream as porosity increased. For porosities above 0.3 the recirculating zone disappeared. Considered as functions of porosity, both the drag coefficient and eddy shedding frequency dropped dramatically at a porosity of about 0.2. Castro concluded that for porosities below 0.2, the shear layers formed at each side of the strip interact to form a vortex street wake. For higher porosities there is sufficient flow through the perforations to eliminate shear layer interactions and prevent the formation of a vortex street, although the wake may "flap" due to a far wake instability.

Experimental Program

Experiments were carried out in the 457-cm long by 134-cm wide by 95-cm high test section of the Purdue Hydromechanics Laboratory low-speed wind tunnel. In the region of measurement, the mean velocity varied by less than 4% in any plane normal to the flow; the freestream turbulence intensity was less than 0.15%; and the static pressure head declined by less than 0.7 mm Hg.[11]

The test objects were 54% scale replicas (2.22-cm wide) of the $\beta=0$ (solid) and $\beta=0.425$ strips used by Castro. The porous strip was covered by a uniform hexagonal pattern of 0.55-cm-diam holes. The strips were mounted normal to the airstream so as to span the test section from floor to ceiling midway between the vertical walls.

Continuous horizontal profiles of mean velocity were obtained using a pitot-static tube mounted on a motorized carriage and connected to a pressure transducer. The speed of traverse (1.2 cm/s) had no effect on the data, and vertical traverses confirmed that the mean flow was two dimensional.

In order to duplicate Castro's conditions, data was gathered at a Reynolds number of 25,000 ($U_\infty = 16.7$ m/s) for both strips. Since the drag coefficient is a function of porosity, the momentum thicknesses of the two strips were not equal. For each strip, horizontal velocity profiles at mid-height were obtained at $x/c=20$, 40, 60, 80, and 100.

According to the constant eddy viscosity theory of the two-dimensional turbulent wake, the centerline velocity defect and characteristic width should vary as the -0.5 and $+0.5$ powers of distance from the virtual origin. Values of ΔU_c and ℓ were obtained from each of the measured profiles. The ΔU_c data were used to fix the position of the virtual origin by fitting a least squares line to $(U_\infty/\Delta U_c)^2$ as a function of x.

$$(U_\infty/\Delta U_c)^2 = 0.111(x+14.78\text{ cm}), \quad r=0.985\ (\beta=0)$$
$$= 0.266(x-12.95\text{ cm}), \quad r=0.990\ (\beta=0.425) \tag{2}$$

The virtual origin is upstream of the solid strip but is downstream of the porous strip. With these virtual origins, least squares lines were fit to the ℓ^2 measurements.

$$\ell^2 = 0.137(x+14.78\text{ cm}), \quad r=0.985\ (\text{solid strip}, \beta=0)$$
$$= 0.044(x-12.95\text{ cm}), \quad r=0.991\ (\text{porous strip}, \beta=0.425) \tag{3}$$

Both Eqs. (2) and (3) provide good fits of the data.

Dimensionless velocity profiles normalized using the ℓ values given by Eq. (3) are plotted in Fig. 1. It is seen that the mean velocity profiles of both strips achieve self-preservation by $x/c=20$. On the other hand, the constant eddy viscosity Gaussian profile overpredicts the velocity defect for $y/\ell<1$ and underpredicts for $y/\ell>1$.

Inasmuch as both wakes have self-preserving mean velocity profiles in the region of measurement, it makes sense to compare their characteristic widths. Equation (3) shows that the solid strip wake spreads more rapidly, but such a comparison is not decisive because the solid strip also has the greater drag. Instead the equations should be normalized using the corresponding momentum thicknesses which are $\theta=2.05$ cm for the solid strip and $\theta=1.18$ cm for the porous strip. These values are based on Castro's extensive wake survey measurements of drag coefficient which he corroborated using a drag balance. The normalized equations

$$\ell/\theta = 0.259(x'/\theta)^{0.5}\ (\text{solid strip}, \beta=0)$$
$$= 0.192(x'/\theta)^{0.5}\ (\text{porous strip}, \beta=0.425) \tag{4}$$

show that the solid strip wake does indeed grow faster than the porous strip wake.

It is of interest to note that Tennekes and Lumley[9] give an equation of the same form but with a coefficient of 0.252 for the circular cylinder, a result that is practically identical with the present solid strip result. This supports the notion that the far wake growth behind solid strips is strongly affected by large eddy shedding as is true for cylinders.

The normalized equations for the centerline velocity defect are

$$\Delta U_c/U_\infty = 2.10(x'/\theta)^{-0.5}\ (\text{solid strip}, \beta=0)$$
$$= 1.78(x'/\theta)^{-0.5}\ (\text{porous strip}, \beta=0.425) \tag{5}$$

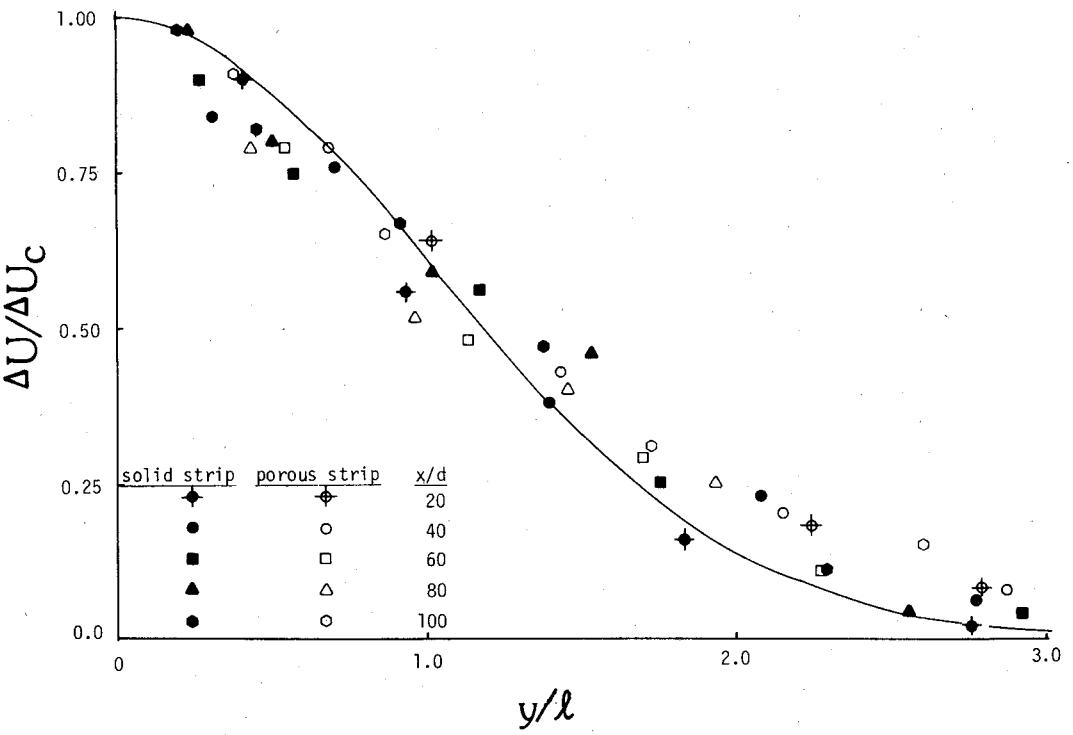

Fig. 1 Normalized velocity defect profiles.

The present results demonstrate that the normalized wake growth behind a solid strip is much faster than behind a porous strip with $\beta = 0.425$. According to the findings of Castro, the wake of the solid strip is dominated by a vortex street which does not form behind the $\beta = 0.425$ porous strip. Taken together, these results indicate that the two-dimensional far wake does depend on the shape of the wake producing object insofar as the shape affects the formation of large vortical structures.

Acknowledgments

The authors gratefully acknowledge the advice of Dr. Paul M. Bevilaqua and thank Prof. Paul S. Lykoudis, Prof. Gerrit H. Toebes, and David L. Cochran for their assistance.

References

[1] Bevilaqua, P. M. and Lykoudis, P. S., "Turbulence Memory in Self-Preserving Wakes," *Journal of Fluid Mechanics*, Vol. 89, Dec. 1978, pp. 589-606.

[2] Hinze, J. O., *Turbulence*, 2nd Ed., McGraw-Hill, New York, 1975, pp. 483-520.

[3] Townsend, A. A., *The Structure of Turbulent Shear Flow*, 2nd Ed., Cambridge University Press, Cambridge, 1976, Chap. 6.

[4] Bevilaqua, P. M. and Lykoudis, P. S., "Entrainment and the Large Eddy Structure," AIAA Paper 75-115, 1975.

[5] Bevilaqua, P. M., personal communication, Aug. 6, 1980.

[6] Brown, G. L. and Roshko, A., "Effect of Density Differences on the Turbulent Mixing Layer," *Turbulent Shear Flows, AGARD Conference Proceedings No. 93*, Paper 23, pp. 1-12.

[7] Papailiou, D. D. and Lykoudis, P. S., "Turbulent Vortex Streets and the Mechanism of Entrainment," *Journal of Fluid Mechanics*, Vol. 62, Jan. 1974, pp. 11-31.

[8] Hwang, N. H. and Baldwin, L. V., "Decay of Turbulence in Axisymmetric Wakes," *Journal of Basic Engineering*, Vol. 88, March 1966, pp. 261-268.

[9] Tennekes, H. and Lumley, J. L., *A First Course in Turbulence*, MIT Press, Cambridge, Mass., 1972, pp. 104-124.

[10] Castro, I. P., "Wake Characteristics of Two-Dimensional Perforated Plates Normal to an Airstream," *Journal of Fluid Mechanics*, Vol. 46, April 1971, pp. 599-609

[11] Sheldon, G. F., "Measurements of Subsonic Wind Tunnel Performance and Two-Dimensional Turbulent Wake Characteristics," MSCE Thesis, Purdue University, 1980, pp. 1-122.

AIAA 82-4016

Acoustic Oscillations in Internal Cavity Flows: Nonlinear Resonant Interactions

L. King Isaacson* and Alan G. Marshall†
University of Utah, Salt Lake City, Utah

EVIDENCE has been accumulating which indicates that the presence of vortex-driven acoustic oscillations may provide a significant contribution to oscillating pressure levels in segmented solid propellant rocket motors. Several years ago, Flandro and Jacobs[1] suggested that periodic vortex shedding could interact with the chamber acoustics to generate pressure oscillations. Culick and Magiawala[2] were able to produce discrete acoustic oscillations in an open-ended flow cavity using both pairs of obstructions and several obstructions in the flow passage. A recent experimental study by Dunlop and Brown[3] indicated that restrictor pairs placed in a choked internal flow can produce significant increases in the magnitude of the pressure oscillations. Their results indicated that not only is the position of the restrictor pair relative to the acoustic mode structure an important parameter, but that the restrictor spacing is also of importance in determining the pressure oscillations produced by vortex shedding and interaction.

This Note presents experimental results which indicate that, for a fixed restrictor pair location and for a fixed restrictor spacing, the primary acoustic oscillation is produced by vortex interaction with the downstream restrictor pair and that significant nonlinear coupling occurs between the internal shear layers produced by the forward restrictor pair and the acoustic pressure field, resulting in resonant acoustic trios of frequency.

The facility used for this study was a subsonic wind tunnel with a test section 2.44 m in length and a cross section of 17.8×17.8 cm. The internal flow cavity consisted of two sets of restrictor pairs as indicated in Fig. 1. The forward plane of the flow cavity was located at a position 79% of the test section length from the entrance to the test section. An X-configuration, constant-temperature, hot-film anemometer system was used to measure axial velocity frequency spectra for various centerline velocities. Two TSI Model 1050 Constant Temperature Anemometers with two TSI Model 1055 Linearizers, together with a TSI Model 1015C Sum and Difference Circuit were used for the velocity measurements. Frequency spectra were obtained with a Hewlett-Packard Model 3590A Wave Analyzer. Analog data acquisition and digital processing were accomplished with a Hewlett-Packard Model 2240A Measurement and Control Processor, a Hewlett-Packard HP-85 Controller, and a Hewlett-Packard Model 7225A Plotter. Figure 2 shows the velocity frequency spectrum for a cavity centerline velocity of 17.6 m/s. The anemometer sensors were located on the cavity centerline directly between the edges of the forward restrictors.

As the velocity is increased, a variety of acoustic frequencies are produced. Figure 3 presents Strouhal number vs flow Reynolds number where the Strouhal number is defined as

$$S = fL/U_0 \tag{1}$$

where f is the frequency, L the length between restrictor pairs, and U_0 the velocity on the centerline between the edges of the forward restrictor pair. Reynolds number is defined as

$$R = U_0 D/\nu \tag{2}$$

where D is the separation distance between the edges of the forward pair of restrictors and ν the kinematic viscosity. Two broad categories of Strouhal number around the values 1 and 2 are readily apparent. However, specific patterns of Strouhal number of each Reynolds number are also apparent. Figure 4 shows a velocity frequency spectrum for a flow Reynolds number of 7.14×10^4 indicating the frequencies giving rise to the corresponding Strouhal numbers in Fig. 3. Note in Fig. 4 that the frequencies fall into the pattern

$$f_1 \pm f_2 \pm f_3 = 0 \tag{3}$$

There are over 20 sets of Strouhal number in Fig. 3 which fit into this pattern.

This type of relationship reflects a condition of resonance produced by a nonlinear quadratic interaction between the various modes of discrete oscillations. The upper and lower shear layers serve as sources of oscillation energy coupling to the pressure wave equation for the inviscid flow along the

Received June 4, 1981.

*Professor, Dept. of Mechanical and Industrial Engineering. Associate Fellow AIAA.

†Graduate Research Assistant, Dept. of Mechanical and Industrial Engineering.